# Modeling Repressor Dynamics and Cooperativity in an *Escherichia coli lac* Operon System

Jorden Smyth, Samantha Ferrao, and Kristiana Nakaj

MATH 5515 Final Project

December 4 2024

## 1 Introduction

### 1.1 Background and Motivation

The *lac* operon, discovered in 1961 [1], is a widely-used example of a prokaryotic molecular control system, and utilizes a negative feedback loop to regulate gene expression pertaining to the uptake and utilization of the disaccharide molecule lactose. It is most commonly studied in the enteric bacterium species *Escherichia coli* (*E. coli*) [2]. The *lac* operon in *E. coli* (Figure 1) contains several key genes, each with distinct functional roles:

- *lacZ*: This encodes $\beta$-galactosidase, an enzyme responsible for breaking down lactose into glucose and galactose.
- *lacY*: This encodes lactose permease, a transporter protein that facilitates the uptake of lactose into the cell.
- *lacA*: This encodes transacetylase, an enzyme assisting in the detoxification of harmful saccharides by removing them from the cell [3].
- *lacI*: This encodes the *lac* operon-specific repressor protein, which inhibits the expression of downstream genes *lacZ*, *lacY*, and *lacA* in the absence of lactose.

The *lac* operon, in its native state, is regulated by the repressor protein coded for by the *lacI* gene. This protein binds to any of the three operator sequences within the operon (*O*1*, O*2*,*

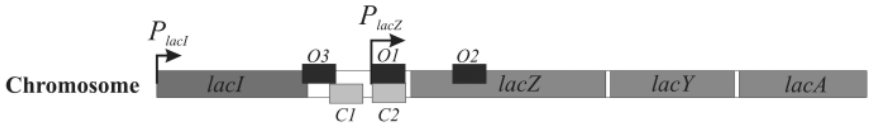


Figure 1: Illustrative diagram of the *lac* operon, from Semsey et. al [2]

*O*3), thereby preventing the RNA polymerase enzyme from transcribing the structural genes (*lacZ*, *lacY*, and *lacA*). When the internal cellular concentration of lactose increases in an *E. coli* cell, a portion of the lactose is converted into allolactose [4]. Allolactose molecules bind to the repressor protein, inducing a conformational change that inhibits its ability to bind to the operator sequences. This change enables the transcription and subsequent expression of the proteins encoded by the structural genes.

While decades of molecular biology research have provided insights into systems like the *lac* operon, numerous experimental limitations remain. For instance, it is challenging to directly measure how rapidly the system responds to changes in lactose availability or predict the outcomes of altered expression levels of key components using empirical methods alone. Mathematical modeling has been employed as a powerful tool to address these challenges. By developing models based on experimental data, researchers can simulate biological systems *in silico*, enabling predictions of system behavior under various conditions. Furthermore, computational approaches allow integration of components from multiple models, reducing reliance on costly, time-consuming and labor-intensive experiments.

Building on these insights, we aimed to replicate a deterministic model of the *lac* operon dynamics, originally described by Semsey et. al. Our study focused on the relationship between external lactose concentration and the average number of lactose permease molecules in an *E. coli* cell, as presented in Figure 3a (Figure 4 in the original study). This analysis utilized a system of ordinary differential equations (ODEs) to capture the dynamics of the *lac* operon, including the autoregulatory feedback mechanism of the LacI repressor. These ODEs only considered the *lacI*, *lacY*, and *lacZ* gene products, hence we did not consider LacA expression for the purpose of our study. In addition, we proposed an extension to the original model by incorporating an assumption of cooperative behavior in the term describing the import of external lactose into the cell. We evaluated the outcomes of both our replicated model and the extended framework against the original

figure and assessed their consistency with the findings reported by Semsey et al.

### 1.2 Research Questions and Extension

The LacI repressor-based feedback mechanism is central to the *lac* operon system and controls lactose utilization in *E. coli*. By dynamically adjusting the expression of structural genes in response to lactose availability, it directly affects the efficiency and responsiveness of the system. Understanding how LacI regulation impacts operon performance provides critical insights into the optimization of lactose metabolism, a process fundamental to bacterial growth and adaptation.

The model developed by Semsey et al. represents *lac* operon dynamics, but it does not account for enzyme cooperativity, a process where substrate binding to one active site affects the ability of an enzyme to bind additional substrates. Without this consideration, the model cannot fully represent non-linear behaviors such as ultrasensitive responses to substrate concentration, which are commonly observed in biological systems. As a result, it may underestimate the sensitivity and dynamic range of the system resulting from fluctuations in lactose availability, oversimplifying key regulatory features.

To address this limitation, we modified the original model by replacing Michaelis-Menten kinetics with Hill-type functions in the relevant equations. The Michaelis-Menten approach assumes independent substrate binding to enzyme active sites, producing a hyperbolic relationship between substrate concentration and reaction velocity. Hill-type functions, by contrast, introduce a Hill coefficient to quantify the degree of cooperativity, enabling the model to account for sharper transition behaviors characteristic of cooperative systems. We expected this modification to yield significant differences in LacY expression patterns, particularly in the sensitivity of the system to the external lactose concentration.

## 2 Methods

### 2.1 Replication of the Deterministic Mathematical Model from the Original Paper

Our approach to replicating the deterministic model of *lac* operon behavior from Semsey et al. involved two key simulation conditions for LacI concentration: (1) a dynamically varying LacI

concentration over time, and (2) fixed LacI concentrations representing low (30 nM) and high (90 nM) regulatory activity.

To replicate this model, we analyzed the concentrations of key components in the *lac* operon system, including internal lactose ($L$), internal allolactose ($A$), LacI mRNA ($I_m$), LacI tetramers ($I$), LacY permeases ($Y$), and LacZ enzymes ($Z$). We made the same assumptions in our replication as in Semsey et al. First, we assumed rapid binding and unbinding of allolactose to LacI, reflecting the fast timescales of molecular interactions in the cell. This enabled us to calculate the concentration of active LacI using the following equation:

$$I^* = \frac{I}{1 + \left(\frac{A}{K_A}\right)^{h_A}} \tag{1}$$

This equation represents the fraction of LacI tetramers that remain active as a function of internal allolactose concentration ($A$), with $K_A$ denoting the dissociation constant for allolactose binding and $h_A$ representing the Hill coefficient for cooperativity. This assumption simplifies the system while preserving its essential regulatory dynamics.

Secondly, we assumed that the binding of LacI to the operator sites ($O1$, $O2$, and $O3$) results in distinct bound states, each associated with specific energy levels that influence their probability of occurrence. Based on these probabilities, we consided only the most likely operator states: (i) no operators bound, (ii) $O1$ bound, (iii) a DNA loop formed between $O1$ and $O2$, and (iv) a DNA loop formed between $O1$ and $O3$. In this context, transcription—the process by which RNA polymerase copies DNA into RNA to produce gene products—is tightly regulated by these operator states [5]. DNA loops are formed when LacI binds simultaneously to two operators, preventing RNA polymerase from accessing the structural genes, thereby repressing their expression.

Finally, we assumed that the effects of LacI and cAMP-CRP on the *lac operon* activity are independent of each other, enabling the rates of change for the *lac* operon (Equation 2) and the *lacI* gene (Equation 3) to be represented as a function of $\epsilon$, where $\epsilon_n$ represents the operator binding

energies (n = 1,2,3):

$$\text{lac activity}(I^*) = \frac{1}{1 + (\epsilon_1 + \epsilon_2 + \epsilon_3)I^*} \tag{2}$$

$$\text{lacI activity}(I^*) = \frac{1 + (\epsilon_1 + \epsilon_2)I^*}{1 + (\epsilon_1 + \epsilon_2 + \epsilon_3)I^*} \tag{3}$$

Under these assumptions, our system includes the following differential equations to deterministically model the *lac operon*:

$$\frac{dL}{dt} = \nu_y Y \left(\frac{L_{ext}}{L_{ext} + K_{ext}}\right) - \nu_y Y \left(\frac{L}{L + \lambda K_{ext}}\right) - 2\nu_z Z \left(\frac{L}{L + K}\right) \tag{4}$$

$$\frac{dA}{dt} = \nu_z Z \left(\frac{L}{L + K}\right) - \nu_z Z \left(\frac{A}{A + K}\right) \tag{5}$$

$$\frac{dI_m}{dt} = k_c \left[\frac{1 + (\epsilon_1 + \epsilon_2)I^*}{1 + (\epsilon_1 + \epsilon_2 + \epsilon_3)I^*}\right] - \gamma_m I_m \tag{6}$$

$$\frac{dI}{dt} = k_l I_m - \gamma I \tag{7}$$

$$\frac{dY}{dt} = k_y \left(\frac{\alpha + \epsilon_C C}{[1 + (\epsilon_1 + \epsilon_2 + \epsilon_3)I^*][1 + \epsilon_C C]}\right) - \gamma Y \tag{8}$$

$$\frac{dZ}{dt} = k_z \left(\frac{\alpha + \epsilon_C C}{[1 + (\epsilon_1 + \epsilon_2 + \epsilon_3)I^*][1 + \epsilon_C C]}\right) - \gamma Z \tag{9}$$

$$\frac{dI_m}{dt} = k_c \left[\frac{1 + (\epsilon_1 + \epsilon_2)I^*}{1 + (\epsilon_1 + \epsilon_2 + \epsilon_3)I^*}\right] - \gamma_m I_m \tag{10}$$

$$\frac{dI}{dt} = k_l I_m - \gamma I \tag{11}$$

$$\frac{dY}{dt} = k_y \left(\frac{\alpha + \epsilon_C C}{[1 + (\epsilon_1 + \epsilon_2 + \epsilon_3)I^*][1 + \epsilon_C C]}\right) - \gamma Y \tag{12}$$

$$\frac{dZ}{dt} = k_z \left(\frac{\alpha + \epsilon_C C}{[1 + (\epsilon_1 + \epsilon_2 + \epsilon_3)I^*][1 + \epsilon_C C]}\right) - \gamma Z \tag{13}$$

Equation 4 models the rate of change of the intracellular concentration of lactose (L). The first term on the right-hand side represents the import of external lactose (or external lactose concentration, $L_{ext}$) by lactose permease (LacY) at maximum rate $\nu_y$, the second term represents the export of internal lactose by LacY, and the final term represents how lactose is used by the enzyme LacZ. The latter term is multiplied by 2 to account for the fact that LacZ can process

lactose in two different ways: hydrolysis and conversion to allolactose both at rate $\nu_z$.

Equation 5 is an expression of the rate of change of the intracellular concentration of allolactose (A), through the production of allolactose and its hydrolysis by LacZ with the same Michaelis-Menten constant K.

Equations 6 and 7 describe the rate of change of the concentration of LacI mRNA ($I_m$) and repressor (I). $k_c$ and $k_l$ are parameters that set the maximal rates of transcription of $I_m$ and translation of I from $I_m$ respectively, while $\gamma_m$ and $\gamma$ set the dilution and degradation rates of $I_m$ and I respectively.

Equation 8 models the rate of change of the concentration of lactose permease (LacY) protein (Y) in the *E. coli* cell, where $k_y$ represents a rate constant for LacY protein translation, the complex term represents the regulation of LacY transcription, and the last term accounts for the degradation of the protein.

Similarly, Equation 9 describes the rate of change of the concentration of LacZ enzyme (Z), where $k_z$ is rate constant for LacZ protein translation, the complex term is identical to the one in Equation 8, and $\gamma$ accounts for the degradation of LacZ.

For our model, we further simplified the system by assuming that the rate of lactose transport and breakdown of lactose and allolactose is greater than the rate of generation of mRNA and proteins. Under this assumption, the amount of lactose and of allolactose in the cell are in quasi-equilibrium. Therefore, by setting $\frac{dL}{dt} = \frac{dA}{dt} = 0$, we mathematically manipulated the original equations for $\frac{dL}{dt}$ and $\frac{dA}{dt}$ to arrive at the following simplified quadratic equation form:

$$c_2 L^2 + c_1 L - c_0 = 0 \tag{14}$$

$$c_0 = \nu_y Y \tilde{L}_{ext} \lambda K K_{ext} \tag{15}$$

$$c_1 = \nu_y Y K (1 - \tilde{L}_{ext}) - \nu_y Y \lambda K_{ext} \tilde{L}_{ext} + 2\nu_z Z \lambda K_{ext} \tag{16}$$

$$c_2 = \nu_y Y (1 - \tilde{L}_{ext}) + 2\nu_z Z \tag{17}$$

$$\tilde{L}_{ext} = \frac{L_{ext}}{L_{ext} + K_{ext}} \tag{18}$$

Solving for $L$, we get:

$$A = L = \frac{1}{2c_2}(-c_1 + \sqrt{c_1^2 + 4c_2c_0}) \tag{19}$$

The above system is a deterministic model of *lac* operon behavior which we utilized to calculate the steady state concentration of LacY in a cell as a function of $L_{ext}$. All the parameters used in this study model are listed in Appendix 6.1. The differential equation system was solved numerically using the **ode45** function in MATLAB R2024b.

## 2.2 Mathematical Model with Hill-Type Behavior of External Lactose Import

In the extension to our study, we assumed cooperation in the term representing the import of $L_{ext}$ into the cell. We modified the first term of Equation 4 to include Hill-function forms, as shown in Equation 17. From this, we derived a new set of equations by again assuming quasi-equilibrium of $\frac{dL}{dt}$ and $\frac{dA}{dt}$ and equating them to each other.

$$\nu_y Y \left(\frac{L_{ext}}{L_{ext} + K_{ext}}\right) \rightarrow \nu_y Y \left(\frac{L_{ext}^n}{L_{ext}^n + K_{ext}^n}\right) \tag{20}$$

$$\frac{dL}{dt} = \nu_y Y \left(\frac{L_{ext}^n}{L_{ext}^n + K_{ext}^n}\right) - \nu_y Y \left(\frac{L}{L + \lambda K_{ext}}\right) - 2\nu_z Z \left(\frac{L}{L + K}\right) \tag{21}$$

This resulted in new equations for $L$ and $A$, while the equations for LacI mRNA, LacI, LacY, and LacZ remained the same under this alteration. The complete derivation is provided in Appendix 6.2.1, and the updated equations are presented below.

$$0 = c2L^2 + c1L - c0 \tag{22}$$

$$c_0 = \nu_y Y \tilde{L}_{ext}^n \lambda K K_{ext} \tag{23}$$

$$c_1 = \nu_y Y K (1 - \tilde{L}_{ext}^n) - \nu_y Y \lambda K_{ext} \tilde{L}_{ext}^n + 2\nu_z Z \lambda K_{ext} \tag{24}$$

$$c_2 = \nu_y Y (1 - \tilde{L}_{ext}^n) + 2\nu_z Z \tag{25}$$

where

$$\tilde{L}_{ext}^n = \frac{L_{ext}^n}{L_{ext}^n + K_{ext}^n} \tag{26}$$

and

$$L = A = \frac{1}{2c_2} - c_1 + \sqrt{c_1^2 + 4c_2c_0} \tag{27}$$

This modification introduced cooperativity into the lactose import process, where the Hill coefficient ($n$) determines the degree of cooperativity [6]. A higher value of $n$ indicates stronger cooperativity, meaning that the binding of one lactose molecule enhances the binding of subsequent molecules.

# 3 Results

## 3.1 Results of Original Model Replication

The solution of the above equation system is graphically presented in Figure 2. Initial conditions of $I_{m_0} = 0.1$ nM, $I_0 = 90$ nM, $Y_0 = Z_0 = 10$ nM, and $L_{ext} = 10^7$ nM were used. Under these conditions, LacI concentration decreases over time, facilitating the expression of LacY and LacZ, as expected with high $L_{ext}$ values.

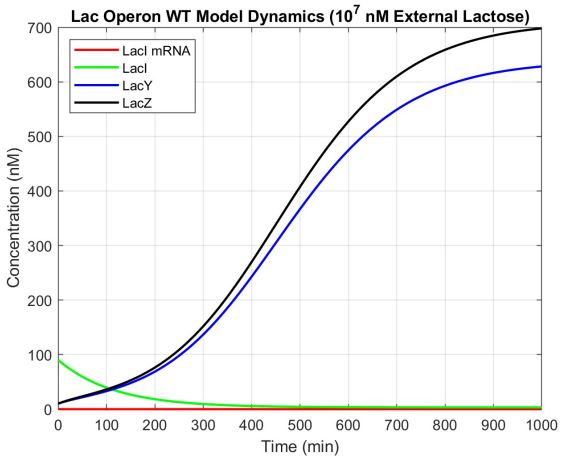


Figure 2: Dynamics of the deterministic mathematical model described in the Methods section. The degradation of LacI enables the production of LacY and LacZ.

The primary objective of this study was to replicate the results from Figure 3a, which demonstrated the variation of steady-state LacY concentration as a function of $L_{ext}$ ($10^3$ nM to $10^5$ nM). In this plot, three scenarios are represented: (1) a fixed-low LacI concentration (30 nM, leftmost curve), (2) the wild-type system (WT), with unrestricted LacI dynamics (middle curve), and (3) a

fixed high LacI concentration (90 nM, rightmost curve). These conditions reflect distinct regulatory states of the *lac* operon. Our replication of this analysis is presented in Figure 3b and shows notable differences in LacY steady-state behavior compared to Figure 3a.

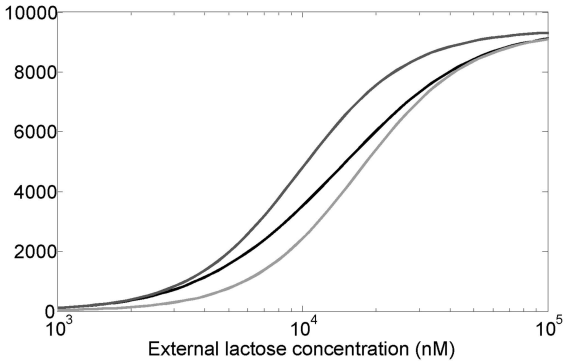


(a) Original results from Semsey et al. [2], illustrating the steady-state LacY expression as a function of $L_{ext}$. The leftmost curve represents the 30 nM "fixed-low" LacI condition, the middle curve shows the wild-type (WT) system, and the rightmost curve represents the 90 nM "fixed-high" LacI condition.

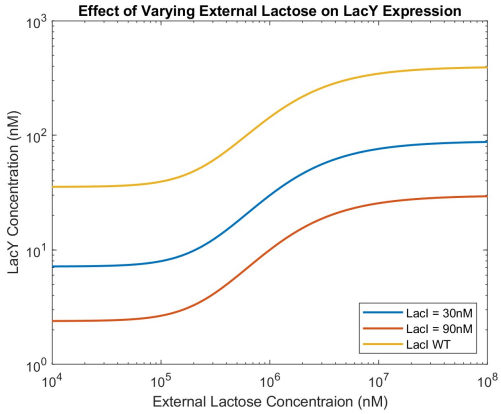


(b) Results from our model replication, showing steady-state LacY expression across varying external lactose concentrations. The curves correspond to 30 nM "fixed-low," 90 nM "fixed-high," and the WT system.

Figure 3: Comparison of steady-state LacY expression as a function of $L_{ext}$.

The main differences observed in our replication include the range of $L_{ext}$ driving system dynamics, the impact of varying LacI levels, and the dynamic range of the system in response to external lactose. In our plot, the most significant changes in steady-state LacY expression occurred over the range of $10^5$ nM to $10^7$ nM, as opposed to the $10^3$ nM to $10^5$ nM range reported in the original study. This shift is consistent with Equation 18 and magnitude of $K_{ext}$. Given that $K_{ext}$ is 0.27 mM (270,000 nM), Equation 18 transitions from near zero at values significantly below $K_{ext}$ to near one at values much higher than $K_{ext}$. Since this equation predominantly drives the dynamics of the system, the changes should occur in the range of $L_{ext} = 10^5$ - $10^7$ nM.

We also observed that, rather than simply converging at a different rate to the same steady-state concentration, varying the LacI level in the system from 30 nM to 90 nM and the WT did not significantly affect the behavior of the system in response to varying $L_{ext}$. Instead, it drastically altered the steady-state concentrations. The WT system exhibited the highest LacY expression levels (ranging from 35 nM to 390 nM), while the fixed LacI systems showed reduced

LacY expression due to the inability of the repressor concentration to decay, as it does in the WT system.

Finally, the original study [2] reported that the WT system had a dynamic range approximately 50% larger than the fixed LacI systems. The dynamic range is defined as the $L_{ext}$ ratio at which 90% and 10% of the maximum LacY are reached. In our simulation, the calculated dynamic ranges were 33.37 for the WT, 33.90 for the fixed-low, and 33.93 for the fixed-high system. Therefore, contrary to the findings of the original paper, the WT system in our model had a negligibly smaller dynamic range compared to the fixed systems.

### 3.2 Results of Extension of Original Model

As described in the Methods section, we then extended the model by incorporating Hill-type equations for $L_{ext}$ to introduce cooperativity into the system dynamics. To explore the effects of cooperativity, we systematically varied the Hill coefficient ($n$) across the values $n = [0.5, 0.75, 1, 1.5, 2, 3, 5]$, based on ranges reported from different enzymes in the literature [6, 7]. We investigated how varying $n$ impacts steady-state LacY levels and the systems sensitivity to $L_{ext}$.

Figure 4 compares the model dynamics of the system with Hill coefficients of 0.5 and 5. While the overall behavior remains similar to the original model, the steady-state concentrations of LacY and LacZ are reduced at lower Hill coefficients. This reduction occurs because lower Hill coefficients result in a broader dynamic range for the system, as shown in Figure 5.

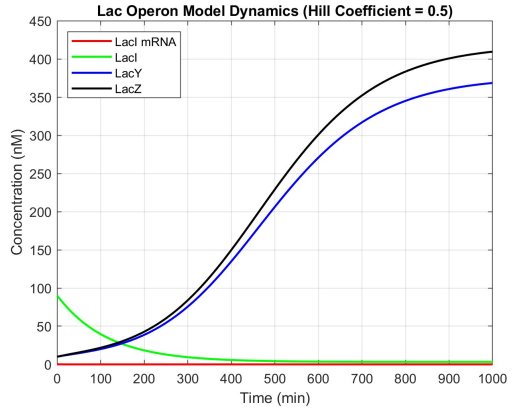


(a) Model dynamics with a Hill coefficient of 0.5, representing lower cooperativity.

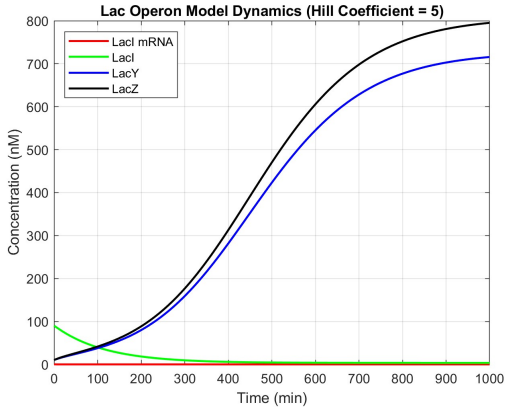


(b) Model dynamics with a Hill coefficient of 5, representing higher cooperativity.

Figure 4: Comparison of model behavior under different levels of cooperativity for external lactose.

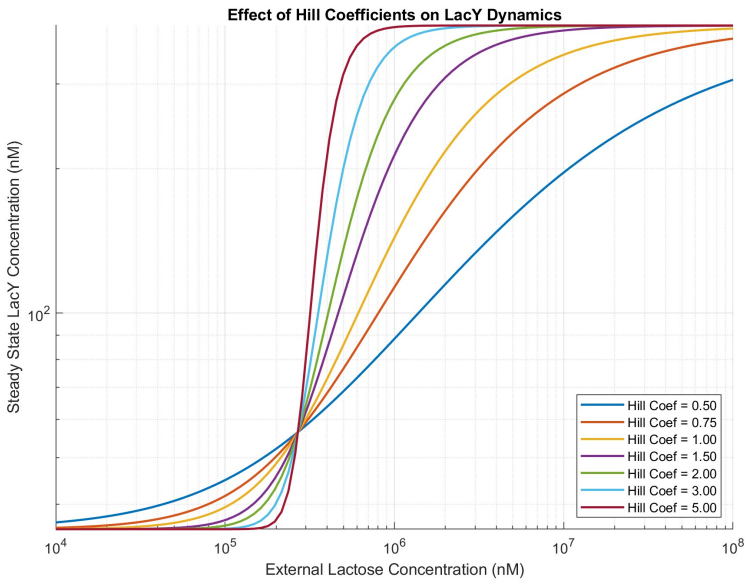


Figure 5: Impact of varying the Hill coefficient on the system's response to increasing external lactose levels. Higher Hill coefficients compress the dynamic range, while coefficients below one expand it.

We further analyzed LacY expression dynamics in response to varying $L_{ext}$ levels across a range of Hill coefficients. Using candidate values of $n = [0.5, 0.75, 1, 1.5, 2, 3, 5]$, Figure 5 shows the behavior of the system at each coefficient value. Our analysis revealed that $L_{ext}$ levels did not significantly affect LacY expression when $L_{ext}$ is either much lower or much higher than $K_{ext}$. Instead, the Hill coefficient influenced the dynamic range of the system.

In our original model ($n = 1$) we calculated a dynamic range of 33.37 using the method described in the Results section. By contrast, a Hill coefficient of 0.5 resulted in a dynamic range of 129.67, while a coefficient of 5 reduced the dynamic range to 2.07. Mathematically, these differences arise from Equation 26, as the rate of transition from zero to one change with the Hill coefficient.

## 4 Discussion

The aim of this paper was to replicate the deterministic mathematical model of the *lac* operon presented by Semsey et al. and extend it by introducing cooperation to the intake of external lactose by adding a Hill coefficient to the initial differential equations. The goal with the extension was to analyze the effect of cooperativity on LacY expression with varying $L_{ext}$ levels. The results

indicated a contrast in the behavior of our system compared to those shown in Figure 3a, and that it had a higher dynamic range, a different magnitude of steady state LacY expression, as well as reacted differently to varying levels of LacI repressor. This extension demonstrated that the introduction of Hill-type structure to the equations for external lactose did not affect the steady state behavior for very small or very large $L_{ext}$ values, but rather impacted the dynamic range. A large Hill coefficient resulted in faster growth and a smaller dynamic range, while vice versa was observed for smaller Hill coefficients.

In the process of creating our model and working to replicate the results found by Semsey et al, we encountered numerous challenges, which included a lack of information about initial conditions, incorrect parameter values, and differing model behavior, which did not align with the mathematical model presented in the original paper. When we initially constructed the model, we noticed that the original paper did not include all the initial conditions that were used for their model. Upon further research, we found what we believe to be reasonable initial conditions, as shown in the results section. However, it is possible that some of the mismatch between our model is due to variations in initial conditions. The mismatch in parameter values included $K_A$ and $K$ having units of $\mu$M, while in the sources cited for them, they were in mM [8]. This led us to question the validity of the other parameter values and spend significant time experimenting with our parameters in an attempt to replicate the behavior of the model. Lastly, as discussed in the results section, the main plot we were replicating (Figure 3a) showed a dynamic range between $10^3$ and $10^5$ nM of external lactose. However, our model had a range between $10^5$ and $10^7$, which corresponds well with the behavior of Equation 18, given that $K_{ext} = 270,000$ nM.

These challenges lead us to believe that there are some significant flaws with the model presented by Semsey et al. If we were to continue work on this model, our next steps would include further research on parameter values, model formulation, and reaching out to the authors to inquire about methods and steps taken that could explain the differences observed in our work.

# 5 Conclusion

While the results we obtained were different from those observed in Semsey et al., the general sigmoidal trends for both fixed and autoregulated LacI levels were successfully replicated. The

extension showed that incorporating Hill-type functions also affects the results, altering the dynamic range of LacY expression to changes $L_{ext}$. Taken together with our proposed future approach, there is potential to further refine the model to produce results similar to WT dynamics found in *E. coli* cells under lactose induction.

# 6 Appendix

## 6.1 Parameter Values

- $\gamma = 0.0087$ min$^{-1}$
- $\nu_y = 2880$ min$^{-1}$
- $\nu_z = 1800$ min$^{-1}$
- $\epsilon_1 = 18/30$ nM$^{-1}$
- $\epsilon_2 = 415.33/30$ nM$^{-1}$
- $\epsilon_1 = 866.66/30$ nM$^{-1}$
- $K_A = 1$ mM
- $K = 1.4$ mM
- $k_c = 1/80$ nM/min
- $\gamma_m = 0.1824$ min$^{-1}$
- $k_y = 90$ nM/min
- $k_z = 100$ nM/min
- $k_l = 90/80$ nM/min
- $\lambda = 750$
- $\frac{\alpha+\epsilon_C C}{1+\epsilon_C C} = 0.9$
- $h_A = 2$
- $K_{ext} = 0.27$ mM

## 6.2 Mathematical Derivations

### 6.2.1 Derivation of Equation set for Extension

Starting by setting equation for $\frac{dL}{dt} = 0$, we can rearrange it into the form of a quadratic.

$$\frac{dL}{dt} = 0 = \nu_y Y \left( \frac{L_{ext}^n}{L_{ext}^n + K_{ext}^n} \right) - \nu_y Y \left( \frac{L}{L + \lambda K_{ext}} \right) - 2\nu_z Z \left( \frac{L}{L + K} \right)$$

Multiply all terms by $(L_{ext}^n + K_{ext}^n)(L + \lambda K_{ext})(L + K)$ to eliminate all denominators.

$$0 = -\nu_y Y L_{ext}^n (L + \lambda K_{ext})(L + K) + \nu_y Y L (L_{ext}^n + K_{ext}^n)(L + K) + 2\nu_z Z L (L_{ext}^n + K_{ext}^n)(L + \lambda K_{ext})$$

Expand each term.

$$\begin{aligned} T1 : &- \nu_y Y L_{ext}^n (L^2 + L(K + \lambda K_{ext}) + \lambda K K_{ext}) \\ T2 : &\nu_y Y (L^2 (L_{ext}^n + K_{ext}^n) + KL(L_{ext}^n + K_{ext}^n)) \\ T3 : &2\nu_z Z (L^2 (L_{ext}^n + K_{ext}^n) + \lambda L K_{ext} (L_{ext}^n + K_{ext}^n)) \end{aligned}$$

Combine terms that contain $L^2$, $L$ or no $L$ and use equation 28 to simplify by dividing all terms by $(L_{ext}^n + K_{ext}^n)$.

$$\tilde{L}_{ext}^n = \frac{L_{ext}^n}{L_{ext}^n + K_{ext}^n} \tag{28}$$

Combine $L^2$ terms, solve for $c_2$.

$$\begin{aligned} c_2 &= -\nu_y Y L_{ext}^n + \nu_y Y (L_{ext}^n + K_{ext}^n) + 2\nu_z Z (L_{ext}^n + K_{ext}^n) \\ c_2 &= \nu_y Y (1 - \tilde{L}_{ext}^n) + 2\nu_z Z \end{aligned}$$

Combine $L$ terms, solve for $c_1$.

$$\begin{aligned} c_1 &= -\nu_y Y L_{ext}^n (K + \lambda K_{ext}) + \nu_y Y K (L_{ext}^n + K_{ext}^n) + 2\nu_z Z \lambda K_{ext} (L_{ext}^n + K_{ext}^n) \\ c_1 &= -\nu_y Y \tilde{L}_{ext}^n K - \nu_y Y \tilde{L}_{ext}^n \lambda K_{ext} + \nu_y Y K + 2\nu_z Z \lambda K_{ext} \\ c_1 &= \nu_y Y K (1 - \tilde{L}_{ext}^n) - \nu_y Y \tilde{L}_{ext}^n \lambda K_{ext} + 2\nu_z Z \lambda K_{ext} \end{aligned}$$

Combine other terms, solve for $c_0$.

$$c_0 = \nu_y Y \tilde{L}_{ext}^n \lambda K K_{ext}$$

## References


[1] M. Lewis, "A tale of two repressors – a historical perspective," *J Mol Biol*, vol. 409, pp. 14–27, May 2011.

[2] S. Semsey, L. Jauffred, Z. Csiszovszki, J. Erdossy, V. Steger, S. Hansen, and S. Krishna, "The effect of lacI autoregulation on the performance of the lactose utilization system in *Escherichia coli*," *Nucleic Acids Research*, vol. 41, p. 6381–6390, July 2013.

[3] K. N. Phillips, S. Widmann, H.-Y. Lai, J. Nguyen, J. C. J. Ray, G. Balázsi, and T. F. Cooper, "Diversity in lac operon regulation among diverse escherichia coli isolates depends on the broader genetic background but is not explained by genetic relatedness," *mBio*, vol. 10, pp. e02232–19, Nov. 2019.

[4] G. Bergstrom, "12.2: Gene Regulation in Prokaryotes- the Lactose (lac) Operon." `https://bio.libretexts.org/Under_Construction/Cell_and_Molecular_Biology_(Bergtrom)/12%3A_Regulation_of_Transcription_and_Epigenetic_Inheritance/12.02%3A_Gene_Regulation_in_Prokaryotes-_the_Lactose_(lac)_Operon`, 2022. [Online].

[5] A. Cournac and J. Plumbridge, "DNA looping in prokaryotes: Experimental and Theoretical Approaches," *Journal of Bacteriology*, vol. 195, no. 6, pp. 1109–1119, 2013.

[6] J. N. Weiss, "The hill equation revisited: uses and misuses," *The FASEB Journal*, vol. 11, p. 835–841, Sept. 1997.

[7] H. Abeliovich, "An empirical extremum principle for the hill coefficient in ligand-protein interactions showing negative cooperativity," *Biophysical Journal*, vol. 89, p. 76–79, July 2005.

[8] M. C. Yildirim, N. Mackey, "Feedback regulation in the lactose operon: a mathematical modeling study and comparison with experimental data.," *Biophysical journal*, vol. 84(5), p. 2841–2851, 2003.